

## Original Research

# Effects of Chronic Diurnal Disruption and Acute Inflammatory Challenge on Mice with Latent Murine Gammaherpesvirus Infection

Rita A Trammell<sup>1</sup> and Linda A Toth<sup>2</sup>

People who engage in shift work (SW) have increased risk of developing illnesses, including infectious diseases and various inflammatory conditions. We hypothesized that exposure to repeated cycles of diurnal disruption, mimicking SW, influences viral clearance, latent viral load, or viral reactivation from latency in mice infected with murine gammaherpesvirus (MuGHV). To test this idea, we inoculated BALB/cByJ and C.129S7(B6)-Ifng<sup>tm1Ts/J</sup> (IFNgKO) mice with MuGHV and housed them under either a stable light:dark (LD) cycle or one mimicking SW. Compared with BALB/cByJ mice, IFNgKO mice generally had higher levels of lytic virus during the 6-wk period after inoculation. In addition, more IFNgKO mice were positive for replicating virus than were BALB/cByJ mice. Exposure to SW did not alter these measures consistently. After the virus had entered the latent phase of infection, mice received either LPS or pyrogen-free saline intraperitoneally. Mice exposed to SW and then injected with LPS during latent infection had greater viral loads and more replicating virus in the lung at 7 d after injection than did either mice that received pyrogen-free saline or those exposed to LD and then treated with LPS. Some cytokine and chemokine concentrations were changed in lung collected 1 d after but not at 7 d after LPS administration. These findings suggest that exposure to repeated chronic diurnal disruption and an acute inflammatory challenge during latent MuGHV infection, in the context of impaired host immune competence, contribute to enhanced viral reactivity and an increased viral load that might trigger ‘sickness behavior’ symptoms of infectious disease and perhaps contribute to chronic fatigue syndrome.

**Abbreviations:** BLI, bioluminescence imaging; EBV, Epstein–Barr virus; LD, light:dark; MuGHV, murine gammaherpesvirus; PFS, pyrogen-free saline; SW, shift work

So-called ‘sickness behaviors’ (for example, fatigue, anorexia, anhedonia, reduced social interaction) have often been linked to facets of the host response to immune or inflammatory challenge. During chronic infections or other chronic inflammatory conditions, the continually primed host immune response is likely to create a powerful and unrelenting stimulus for these debilitating symptoms in at least some patients. Such symptoms might be mediated in part by immune activation or dysfunction, neural–endocrine homeostatic imbalance, or both, as produced secondary to the acute and chronic viral infection.<sup>13,52</sup> Statistical modeling approaches have indicated how a persistent viral infection could theoretically lead to a state of chronic humoral and cellular immune activation.<sup>2</sup> This state was described as a conditional reflex phenomenon in which persistent or repeated exposure to an antigenic stimulus leads to strong reinforcing interactions of B and T cells, ultimately resulting in sustained immune activation even in the absence of the initial eliciting stimulus.<sup>2</sup>

Epstein–Barr virus (EBV) is a ubiquitous human gammaherpesvirus that causes acute disease, establishes life-long latency, and

is associated with the common human syndrome of infectious mononucleosis. Infection with or reactivation of EBV in humans is often associated with fatigue and excessive sleepiness.<sup>1,25,30,39,65,73</sup> Similar findings have been reported for other viral pathogens. For example, among patients with West Nile Virus infection, both proinflammatory and antiviral cytokines were significantly higher in those reporting fatigue as compared with those not reporting fatigue.<sup>21</sup> Studies demonstrating that antibodies to latent EBV proteins are elevated in some patients with chronic fatigue have led to speculation that 1) synthesis of these viral proteins reflects reactivation of latent virus<sup>23,29,45</sup> and 2) although host responses to reactivation may abort viral replication, the viral proteins themselves or the resultant host immune response may trigger or exacerbate fatigue.<sup>24</sup> Furthermore, at least a subset of patients with the condition known as chronic fatigue syndrome appears to have deficient EBV-specific B- and T-cell memory responses, suggesting an impaired ability to control early steps of viral activation.<sup>37</sup>

Gammaherpesviruses, including EBV, are highly species-specific. Murine gammaherpesvirus (MuGHV) is a natural pathogen of wild rodents that provides an experimental model for studying the pathophysiology of an EBV-like pathogen in laboratory mice, which are a permissive host.<sup>18,20,48</sup> The immune response

Received: 05 Apr 2016. Revision requested: 28 Apr 2016. Accepted: 12 Jun 2016.  
Departments of <sup>1</sup>Internal Medicine and <sup>2</sup>Pharmacology, Southern Illinois University  
School of Medicine, Springfield, Illinois  
\*Corresponding author. Email: Toth.linda@frontier.com

of mice to MuGHV infection has been well described.<sup>5,62</sup> After intranasal infection of immune-competent mice with MuGHV, pulmonary viral titers peak between days 6 through 9, and lytic virus is cleared from the lung in about 10 to 14 d.<sup>17</sup> Like other herpesviruses, MuGHV can maintain lifelong latency in its host. Latent virus is established in lung within days after infection.<sup>17</sup> Spleen, lymph nodes, and bone marrow also harbor latent virus, primarily in B lymphocytes.<sup>16-18,63</sup> The number of latently infected cells peaks at approximately day 14 after infection and then falls rapidly.<sup>10</sup> Latent virus persists lifelong under immune control in various cell types, notably B lymphocytes and macrophages.

Our past work has shown that MuGHV-infected mice develop sleep perturbations and behavioral fatigue during the acute lytic phase of the infection; these symptoms resolve as the virus becomes latent yet return with exposure to a secondary challenge (inflammatory challenge, novel social interactions, sleep disruption).<sup>22,49,66,67</sup> A growing literature indicates that disruption of sleep and circadian rhythms in turn disrupts immune and inflammatory responses, increasing risk and exacerbating the severity of a wide range of health conditions.<sup>46,55,58,68</sup> Long-term exposure to shift work (SW) and jet lag have been associated with health problems that include cancer and neurologic, gastrointestinal, metabolic, autoimmune, and cardiovascular disease.<sup>12,26,40,43,51,56,71</sup> We hypothesized that host immune impairment or exposure to chronic diurnal disruption would alter viral clearance, latent viral load, or the initiation or completion of latent virus reactivation in MuGHV-infected mice. To test this idea, we infected mice with MuGHV and then exposed them to chronic repeated diurnal disruption designed to mimic a human SW schedule. During the latent phase of the infection, we further administered an acute inflammatory challenge (LPS). We compared 2 strains of mice—BALB/cByJ and C.129S7(B6)-Ifng<sup>tm1Ts</sup>/J (IFNgKO). Because IFN $\gamma$  is an important component of host defense during MuGHV infection, particularly in BALB/c mice,<sup>69</sup> we considered IFNgKO mice with a BALB/cByJ genetic background as likely to be particularly susceptible to the adverse consequences of viral infection in the context of concurrent diurnal (SW) and immunologic (LPS) challenges. Dependent measures in our study included viral clearance, viral load, and inflammatory markers in lung.

## Materials and Methods

**Mouse procurement and care.** Male and female BALB/cByJ mice (age, 4 to 5 wk) were purchased from the Jackson Laboratory (Bar Harbor, ME). C.129S7(B6)-Ifng<sup>tm1Ts</sup>/J (stock number 002286; IFNgKO) were purchased from the same vendor at the same age for use as breeder stock. Breeders were maintained under barrier conditions as trios of one male and 2 females. Offspring were weaned into same-sex groups and transferred to environmental chambers for housing during experimental use. BALB/cByJ mice were housed in environmental chambers on receipt. Chambers were not light-tight due to a 2-in. opening that permitted cables to exit the chamber. To avoid variation, room lights remained on at all times by design, and chamber doors were opened only during the light phase. Room light intensity was approximately 175 lx. Within chambers at cage level with the chamber door closed, light intensity was approximately 5 to 10 lx during the dark phase (chamber internal lighting off) and 125 to 145 lx during the light phase (chamber internal lighting on).

Internal chamber temperatures were maintained at  $25 \pm 1$  °C. Mice were housed in standard filter-topped cages (12 in.  $\times$  7.5 in.

$\times$  5 in.; 90 in.<sup>2</sup> of floor space) on wood-chip bedding (Beta-Chips, Gateway Supply Company, St Louis, MO). Food (Purina Lab Diet 5008, PMI, St Louis, MO) and tap water (City Light, Water, and Power, Springfield, IL) were available to the mice at all times. Light cycles varied with experimental group. Mice were assumed to be free of standard adventitious pathogens in light of procurement from a reputable vendor and maintenance in areas free of such organisms, as documented by scheduled testing of sentinel animals maintained in the same room. All procedures involving animals were approved in advance by the Laboratory Animal Care and Use Committee of the Southern Illinois University School of Medicine.

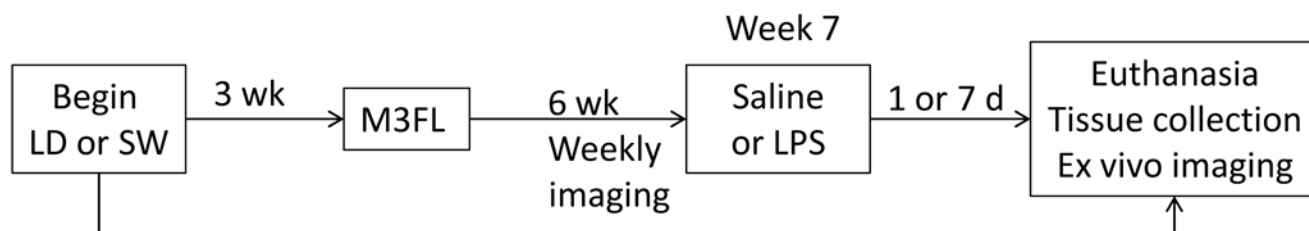
**Experimental design (Figure 1).** Mice were assigned at 5 wk of age to either a stable 12:12-h light:dark (LD) cycle or to a schedule of repeated phase shifts that were designed to mimic SW (Figure 2). Thus, on the first day of the 'work week,' the active (dark) phase was extended by 8 h. This 'shifted' cycle was maintained for the next 4 d. On day 6 (the beginning of the simulated weekend), the onset of the dark (active) phase was advanced by 8 h, thus returning to the control cycle. After 2 'weekend' days, the cycle began again. This pattern was continued for the duration of the study for all mice in the SW groups.

Throughout the study, all animal manipulation (experimental and husbandry) was performed immediately after light onset. In addition, all measurements and husbandry activities were performed on the same day of the week for all mice in the study. The day of the week was selected to coincide with the second weekend day for SW mice. This day was scheduled by design to occur on a Friday. In this way, all mice were on the same LD cycle when caging or experimental manipulations were performed. In addition, mice were checked daily by opening the chamber door during the light phase and visually examining the mice through the cage. Mice were not otherwise disturbed.

At 8 wk of age (after 3 wk of exposure to SW or stable LD conditions), mice were inoculated intranasally under light isoflurane anesthesia with 5000 pfu of virus diluted in 25  $\mu$ L of sterile saline. We used M3FL, a recombinant MuGHV that expresses a firefly luciferase reporter; this virus was constructed and kindly provided by Dr Ren Sun (University of California, Los Angeles, CA.).<sup>27</sup> Viral stocks were produced and quantified according to standard procedures.<sup>10</sup>

The M3FL virus allowed us to use bioluminescence imaging (BLI) to noninvasively and repetitively monitor in vivo viral replication in the same animal over time and to evaluate lytic virus in tissues collected after euthanasia. Viral bioluminescence was monitored in vivo at weekly intervals for 6 wk, beginning on day 7 after inoculation. On day 48 or 49 after infection (that is, during the latent stage of infection), mice were injected intraperitoneally with either 15  $\mu$ g of LPS (*E. coli* O111:B4; Sigma-Aldrich, St. Louis, MO) in 100  $\mu$ L of sterile pathogen-free saline (PFS) or with 100  $\mu$ L of PFS alone. Mice were euthanized 24 h or 7 d after the injection by exsanguination under isoflurane anesthesia. Lungs were collected for ex vivo bioluminescence imaging and then were snap-frozen in liquid nitrogen and stored at  $-80$  °C until processed further.

**BLI.** BLI of M3FL in live mice and harvested organs was performed by using the IVIS-100 imaging system (Xenogen, Alameda, CA). Data acquisition and analysis were performed by using Living Image software version 4 (Xenogen). For in vivo imaging, mice received an intraperitoneal injection of D-luciferin (150 mg/kg;



Continue on assigned light cycle throughout.

**Figure 1.** Experimental design. Mice used in this study underwent the schedule of interventions shown here. Approximately 3 wk after assignment to a test group (LD or SW), mice underwent intranasal administration of M3FL under isoflurane anesthesia. Mice were then monitored weekly for 6 wk by using bioluminescence imaging. On days 48 to 49, mice were injected intraperitoneally with either LPS or pyrogen-free saline; mice were euthanized 1 d after injection for measurement of lung cytokines and chemokines or at 7 d after injection for harvest and imaging of lung tissue and measurement of viral load, cytokines, and chemokines.

	Shift work paradigm (clock time)											
	0000-0200	0200-0400	0400-0600	0600-0800	0800-1000	1000-1200	1200-1400	1400-1600	1600-1800	1800-2000	2000-2200	2200-2400
Day 1 begin work week							8 h delay in sleep (light) phase					
Day 2 work												
Day 3 work												
Day 4 work												
Day 5 work												
Day 1 weekend	8 h advance in active (dark) phase											
Day 2 weekend												E
	Stable LD cycle (clock time)											
	0000-0200	0200-0400	0400-0600	0600-0800	0800-1000	1000-1200	1200-1400	1400-1600	1600-1800	1800-2000	2000-2200	2200-2400
Day 1 work												
Day 2 work												
Day 3 work												
Day 4 work												
Day 5 work												
Day 1 weekend												
Day 2 weekend												E

**Figure 2.** Paradigm for diurnal phase shift to mimic shift work. Gray boxes indicate the dark phase. Mice were euthanized (E) immediately before dark onset at the end of the simulated weekend.

Gold Biotechnology, St Louis, MO.) from a 15 mg/mL stock solution in sterile Dulbecco PBS. Beginning at 5 min after injection of substrate, mice were anesthetized with 4% isoflurane mixed with oxygen and then maintained under 2% isoflurane mixed with oxygen during imaging. BLI was performed to detect signal on 3 views (dorsal, ventral, and left lateral sides) of each mouse. A grayscale surface image of each mouse was obtained at a 1.5-cm

subject-height focus, 12.5-cm field of view, 0.2-s exposure time, medium binning, and 16 f-stop. Overlapping BLI were acquired at the same field of view with a 5-min exposure time, 1 f-stop, medium binning, and an open emission filter. For ex vivo imaging of tissues, mice were euthanized 15 min after intraperitoneal injection of D-luciferin (150 mg/kg). Lung was harvested, and then bioluminescent and grayscale surface images were acquired

at the same settings as used for in vivo imaging except that the field of view was reduced to 5 cm.

**Quantification of luciferase activity.** Relative intensities of bioluminescence were visualized as overlapping pseudocolor images from violet (least intense) to red (most intense). Gray-scale photographs and corresponding color images were superimposed by using Living Image software (Xenogen). Regions with signal above background were identified and quantified by the program, with visual confirmation in a blinded manner. The software expressed the bioluminescent intensity of each targeted region in terms of photon flux (photons/s/cm<sup>2</sup>/steradian), which reflects lytic or replicating virus.<sup>14</sup> For in vivo imaging, values of photon flux were obtained with the mouse lying in each of 3 positions (dorsal, ventral, and left lateral recumbent); these values were summed for analysis. For ex vivo imaging, lung was imaged only from the dorsal surface.

**Viral load.** DNA was isolated from the lungs of infected mice by using DNeasy Blood and Tissue Isolation Kits (Qiagen, Frederick, MD) as described by the manufacturer. Viral load was quantified by real-time PCR as described previously.<sup>72</sup> Primers and probes were designed by using Primer Express Software (PE Applied Biosystems, Foster City, CA) to detect a 70-bp region of the MHV68 gB gene: forward primer, 5' GGC CCA AAT TCA ATT TGC CT 3'; reverse primer, 5' CCC TGG ACA ACT CCT CAA GC 3'; probe, 5' 6-(FAM)-ACA AGC TGA CCA CCA GCG TCA ACA AC-(TAMRA) 3', where FAM is a reporter dye and TAMRA a quencher dye. Each reaction contained 100 ng DNA, TaqMan Universal PCR Master Mix (Applied Biosystems) with 250 nM primers and 200 nM of FAM-Black Hole Quencher-1-labeled probe (Integrated DNA Technologies, Coralville, IA). Samples were subjected to 2 min at 50 °C, 10 min at 95 °C, and 40 cycles of 15 s at 95 °C and 1 min at 60 °C (StepOnePlus Real-Time PCR System, Thermo Fisher Scientific, Waltham, MA). Standard curves were generated by using known amounts of plasmid containing the gB PCR fragment mixed with 100 ng DNA from naïve lung. The copy number of viral genomes in the sample was calculated according to the linear regression of the standard curve generated from the cycle threshold over log<sub>10</sub> copy number. The DNA copy number was calculated from the molecular weight of the DNA construct and Avogadro's number.

**Cytokine and chemokine measurement.** Snap-frozen right lungs were homogenized in 10 volumes (w/v) of ice-cold sterile PBS containing Complete Protease Inhibitor Cocktail (Roche, Camarillo, CA) by using a hand-held polytron homogenizer. Homogenates were centrifuged at 13,700 × *g* at 4 °C for 10 min. An aliquot of supernatant was removed and assayed for protein concentration (BCA Protein Assay, Pierce Scientific, Rockford, IL). The remaining supernatant was stored in aliquots at -80 °C until analysis.

Cytokines and chemokines were measured by using multiplex bead-based assays as described by the manufacturer (MPXMCY-TO-70K, EMD Millipore, Billerica, MA) and were analyzed on a 100IS system (Luminex, Madison, WI) with Bio-Plex Manager 5.0 software (BioRad, Hercules, CA). Minimal detectable concentrations (pg/mL) for individual analytes were 2.0 for IL1β, 1.8 for IL6, 5.3 for MCP1, 5.6 for GCSF, 0.6 for IP10, and 1.4 for KC. The intraassay percentage coefficient of variance ranged from 5.8% (MCP1) to 10.4% (IL6); the interassay percentage coefficient of variance ranged from 4.4% (MCP1) to 10.9% (KC). Samples were assayed in duplicate, normalized to protein concentrations and reported as pg/mg protein for lung homogenates.

**Statistics.** Data were log-transformed prior to analysis due to the nonnormal distribution of values.<sup>50</sup> Descriptive statistics are expressed throughout as mean ± SEM. Comparisons with *P* values of less than 0.05 are reported. SPSS Statistics version 22 (IBM, Armonk, NY) was used for all data analysis.

Cytokine and chemokine concentrations that were below the assay limits of detection were assigned the minimal detectable concentration for purposes of statistical analysis. Concentrations measured in lung tissue collected at 24 h or 7 d after LPS or PFS administration were analyzed separately by using preplanned independent *t* tests. Three comparisons were made: LD and SW groups after saline administration, LD mice after saline or LPS administration, and SW mice after saline or LPS administration.

BLI data from harvested lung tissue and PCR viral load data in the lung were compared by using one-factor ANOVA. When significant effects were detected, preplanned independent *t* tests were used for follow-up. In vivo BLI data in each organ were analyzed by using 3-factor ANOVA (mouse strain [BALB/cByJ or IFNγKO], treatment [PFS or LPS], and light cycle [SW or LD]) to test the overall model at each time point. Step-down 2-factor ANOVA was then used to determine effects of treatment and light cycle within each mouse strain and within sex. When significant effects of mouse strain, sex, treatment, or light cycle or significant interactions were detected, specific comparisons were performed by using one-factor ANOVA with Tukey follow-up to identify significant differences between groups. Proportions of mice showing replicating virus (that is, any degree of bioluminescence) in a given organ were compared by using the Pearson chi square test.

## Results

**Clearance of lytic virus.** Female BALB/cByJ and IFNγKO mice that were exposed to either LD or SW beginning at 3 wk before viral inoculation were evaluated for viral replication and dissemination by weekly BLI for 6 wk beginning at 1 wk after inoculation. Lytic viral load was quantified in 6 tissues (nares, lung, cervical lymph nodes, spleen, vaginal region, and joints) as photon flux (Figure 3, left panel). In addition, the proportion of mice showing the presence of lytic virus in each tissue at each time point was reported (Figure 3, right panel).

In both strains of mice, lytic viral load in each organ and the proportion of mice affected peaked in nares and lung at 1 wk, in cervical lymph nodes and spleen at 2 wk, and in vaginal area at 3 wk after inoculation. By 6 wk after inoculation, lytic virus had been cleared from all infected organs, on the basis of absence of bioluminescence, with the exception of various joints in some mice, which remained positive at that time. IFNγKO mice in general had a significantly (*P* ≤ 0.05) higher peak lytic viral load and a greater proportion of mice affected than did BALB/cByJ mice exposed to the same conditions (Figure 3), but these measures were not significantly affected by exposure to SW. IFNγKO mice showed no significant differences in viral clearance or proportion of mice affected as a function of sex under either LD or SW conditions (data not shown).

**Lung response to secondary inflammatory challenge.** On day 48 or 49 after viral inoculation (that is, during latent viral infection), BALB/cByJ and IFNγKO mice received intraperitoneal injections of LPS or an equivalent volume of PFS; 7 days later, mice received an injection of D-luciferin and were euthanized by anesthetic overdose 15 min later. Lungs were removed for BLI. Three-factor ANOVA revealed that treatment with LPS significantly increased

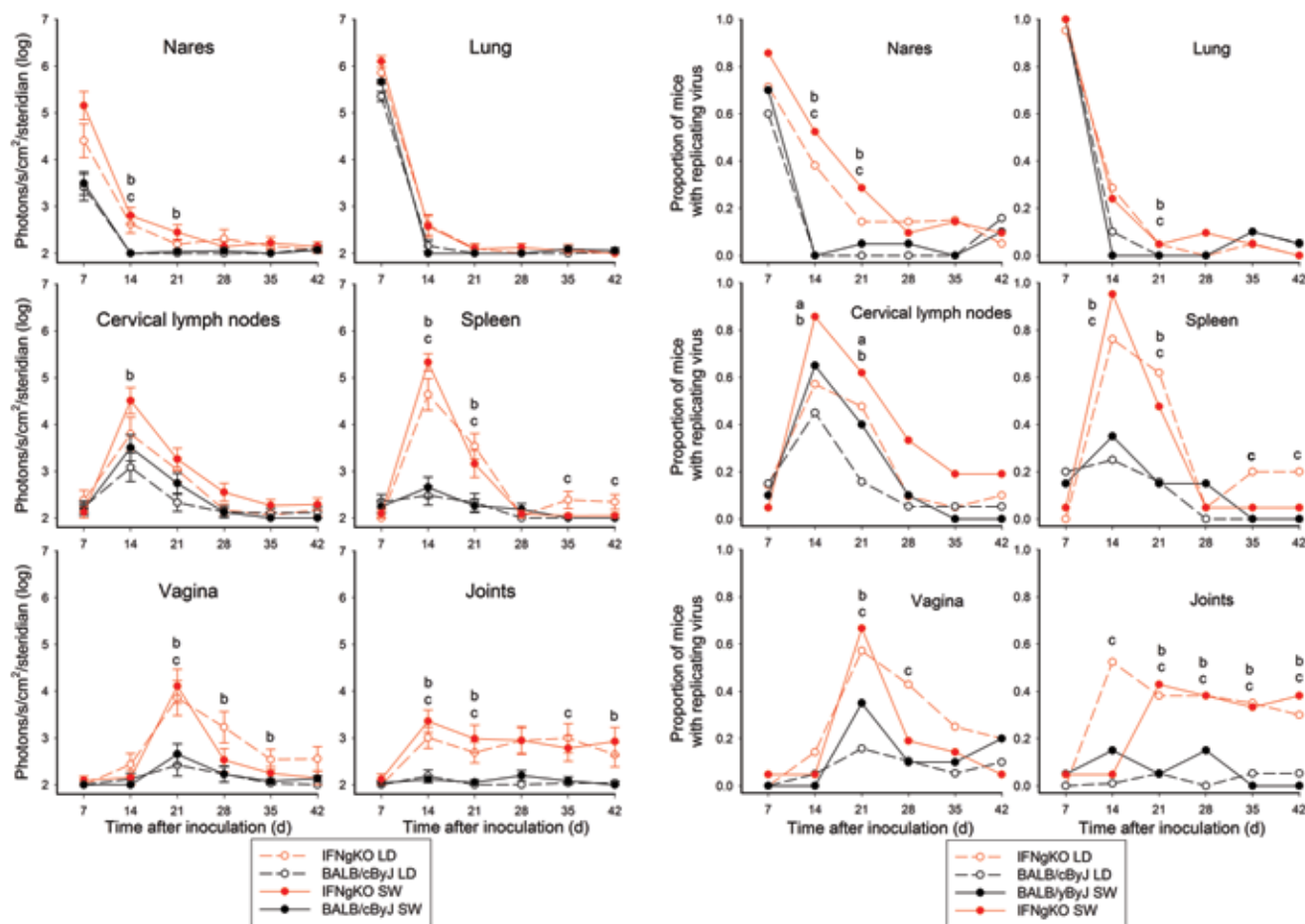


**Figure 3.** Time course for replicating virus in M3FL-infected female BALB/cByJ and IFNgKO mice exposed to stable light:dark (LD) or simulated shift work (SW) conditions. Photon flux (left panels; photons/s/cm<sup>2</sup>/steradian) and the proportion of mice with detectable replicating virus (right panels) were evaluated weekly after intranasal inoculation of BALB/cByJ mice (black symbols and lines) and IFNgKO mice (red symbols and lines) with M3FL ( $n = 20$  mice per group [the 4 groups were BALB/cByJ+LD; BALB/cByJ+SW; IFNgKO+LD; and IFNgKO+SW]). Open symbols show data from mice maintained on stable LD cycles, whereas filled symbols show mice maintained on simulated SW. Six tissues were analyzed: nares, cervical lymph nodes, lung, spleen, vagina, and joints. Intensity data were analyzed by using one-factor ANOVA at each time point. The proportion of mice with detectable replicating virus was analyzed by using Pearson  $\chi^2$  tests. For all analyses,  $P \leq 0.05$  was considered to represent a statistically significant effect, as follows: a, IFNgKO-SW > IFNgKO-LD; b, IFNgKO-SW > BALB/cByJ-SW; c, IFNgKO-LD > BALB/cByJ-LD.

photon flux in lung ( $P = 0.002$ ; Figure 4, top panels), with no significant effects of strain or light cycle. Follow-up independent  $t$  tests within strains revealed that LPS, as compared with PFS, induced a significant increase in lytic virus as measured by photon flux in SW mice but not in LD mice ( $P = 0.011$  for both strains).

Viral load was measured in lungs collected at 7 d after LPS or PFS administration (Figure 4, bottom panels). Three-factor ANOVA (light cycle, treatment, and strain) revealed significant effects of all 3 factors on lung viral load ( $P \leq 0.001$  for each). Follow-up independent  $t$  tests within strain revealed that among BALB/cByJ mice exposed to SW, LPS treatment was associated with a significantly greater ( $P = 0.001$ ) total lung viral load. In contrast, total lung viral load was not significantly altered in LD mice treated with LPS (Figure 4, bottom panels). Among IFNgKO mice, those exposed to SW had significantly greater viral loads after PFS than did LD mice after PFS ( $P = 0.021$ ). Both LD and SW mice treated with LPS had significantly greater viral loads than did the counterpart LD and SW mice treated with PFS ( $P = 0.004$  and  $0.032$  for LD and SW mice, respectively). Viral load showed a trend ( $P$

$= 0.054$ ) toward a statistically significant difference between SW and LD IFNgKO mice at 7 d after administration of LPS.

Lungs were collected from IFNgKO mice at 24 h or 7 d after intraperitoneal administration of LPS or PFS for measurement of cytokine and chemokine concentrations. As compared with LD mice that received PFS, SW mice that received PFS showed significantly lower concentrations of several lung cytokines and chemokine concentration at the 24-h time point. At the 24 h time point, treatment with LPS resulted in significantly higher concentrations of GCSF, IP10, KC, and MCP1 than did treatment with PFS (Figure 5, left panel;  $P < 0.05$  for all). In contrast, the concentrations of these substances did not differ between PFS- and LPS-treated mice at 7 d after LPS administration (Figure 5, right panel). A comparison of values obtained from male and female mice of both strains at 24 h after administration of LPS or PFS revealed no significant effects of sex (data not shown).

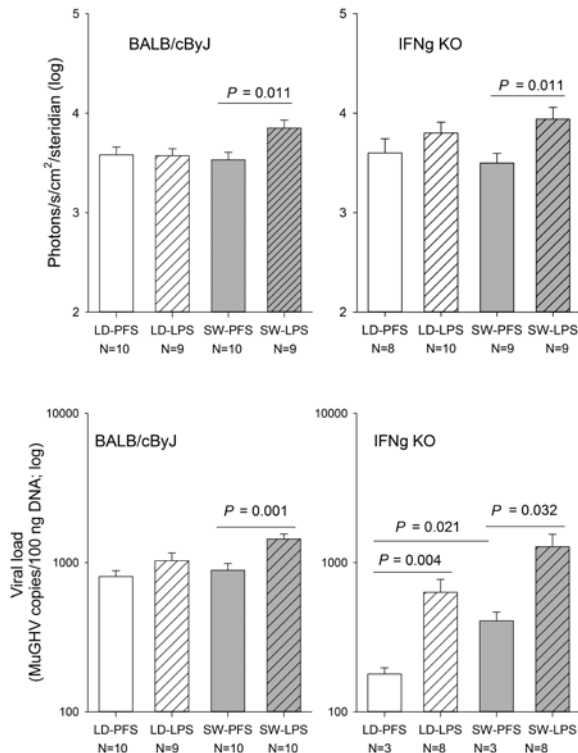


**Figure 4.** Effect of LPS administration on lung viral load in M3FL-infected BALB/cByJ and IFN $\gamma$ KO mice exposed to stable LD or simulated SW conditions. On day 7 after intraperitoneal administration of LPS (15  $\mu$ g) or an equivalent volume of PFS, female BALB/cByJ and IFN $\gamma$ KO mice with latent M3FL infection were intraperitoneally injected with D-luciferin (150 mg/kg), followed 15 min later by euthanasia. Lung tissue was collected and immediately imaged by BLI to quantify the replicating viral load (top panel). Lung tissue was then frozen and later assayed for total lung viral load by using real-time PCR analysis.

## Discussion

This study was designed to determine whether chronically repeated diurnal disruption, mimicking SW, altered viral clearance, influenced the level of latent virus, or exacerbated the response to a secondary inflammatory challenge (LPS), potentially promoting viral or immunologic reactivation and thereby contributing to persistent long-term susceptibility to fatigue. We tested the hypotheses that diurnal disruption of mice with MuGHV infection increases replicating virus titers or delays clearance of virus during acute infection or promotes reactivation of latent virus in mice exposed to LPS. We compared 2 strains of mice—genetically replete BALB/cByJ mice and IFN $\gamma$ -deficient BALB/cByJ mice—in light of the hypothesis that the immune-impaired IFN $\gamma$ KO mice are less able to clear active virus or control latent virus and therefore are more susceptible to SW-related influences on viral clearance and reactivation. IFN $\gamma$  is an important effector mechanism in the clearance of MuGHV; wild-type BALB/C mice can clear infectious MuGHV from the lungs even after high-dose infection, whereas BALB/C mice that lack IFN $\gamma$  have increased viral titers in the lungs on day 10 after infection, as do wild-type BALB/C mice given IFN $\gamma$  blocking antibody.<sup>69</sup> Furthermore, explanted peritoneal cells from infected mice that are deficient in IFN $\gamma$  or the IFN $\gamma$  receptor reactivate more efficiently than do cells collected from IFN $\gamma$ -replete mice.<sup>61</sup> In addition, treatment with IFN $\gamma$  inhib-

its reactivation of MuGHV from latently infected wild-type peritoneal cells, and depletion of IFN $\gamma$  from wild-type mice increases the efficiency of reactivation of explanted peritoneal cells.<sup>61</sup>

Our findings can be summarized as follows. First, in both strains of mice, the proportion of mice affected and the lytic viral load in each organ peaked in nares and lung at 1 wk, in cervical lymph nodes and spleen at 2 wk, and in vagina at 3 wk after inoculation, and lytic virus was cleared from all infected organs, with the exception of some joints in IFN $\gamma$ KO mice. IFN $\gamma$ KO mice, in general, had a higher peak lytic viral load and a greater proportion of mice affected than did BALB/cByJ mice exposed to the same conditions. Neither mouse sex nor exposure to SW affected these measures. Second, at 7 d after injection, LPS administration, as compared with PFS, was associated with a higher level of lytic virus in lung, quantified by BLI, in SW mice but not in LD mice. Third, BALB/cByJ mice exposed to SW and LPS treatment had a significantly higher total lung viral load at 7 d after challenge, whereas total lung viral load was not significantly altered in LD mice treated with LPS. Among IFN $\gamma$ KO mice, SW mice given PFS had greater viral loads than did LD mice treated with PFS. Both LD and SW mice treated with LPS respectively had greater viral loads than did LD and SW mice treated with saline. Fourth, at the 24-h time point after treatment, LPS administration was associated with higher concentrations of GCSF, IP10, KC, and MCP1 than was administration of PFS. In contrast, concentrations of these substances were not significantly different in PFS- and LPS-treated mice at 7 d after LPS administration and were not altered after exposure to SW or LD. These findings suggest that exposure to diurnal disruption in association with an inflammatory challenge can precipitate reactivation of latent virus and an increase in viral load, thereby perhaps triggering the development of fatigue and perhaps other symptoms of infectious disease.

Our data on MuGHV clearance in IFN $\gamma$ -replete and -deficient mice confirm and extend previous findings regarding the role of IFN $\gamma$  in promoting viral clearance and reducing viral load.<sup>61,69</sup> The data present a complete *in vivo* time course of viral clearance across multiple organ systems, showing higher peak titers but not delayed clearance as a function of IFN $\gamma$  deficiency. However, others have reported a slight delay in viral clearance in IFN $\gamma$ KO BALB/cByJ mice.<sup>59</sup> Exposure to simulated SW did not affect viral clearance, although SW was associated with higher peak titers in some tissues at some time points. We conclude that despite the many known physiologic and immunologic repercussions of short- and long-term sleep disruption,<sup>4,38</sup> the specific circadian disruption we imposed did not physiologically or clinically compromise the host's ability to control the acute infection.

Our study also confirmed the previously reported nasal, cervical lymph node, and vaginal distribution of lytic virus in female mice.<sup>19,42</sup> We further observed persistent lytic infection in the joints of some IFN $\gamma$ KO mice (Figure 3). Joint involvement has also been reported to occur during EBV and cytomegalovirus infections in some human patients, in association with inflammation and pain.<sup>15,41,64</sup> Studies of male C57BL/6j mice found that weekly 12-h phase shifts for 22 wk were associated with osteoarthritic changes at several locations, most notably the knee joint.<sup>34,35</sup> In our study, mice with affected joints showed no overt signs of joint inflammation or pain, although BLI detected lytic infection in some joints for as long as 6 wk after inoculation.

We assessed mice at 1- and 7-d intervals after administration of the toll-like receptor 4 ligand LPS; others have determined

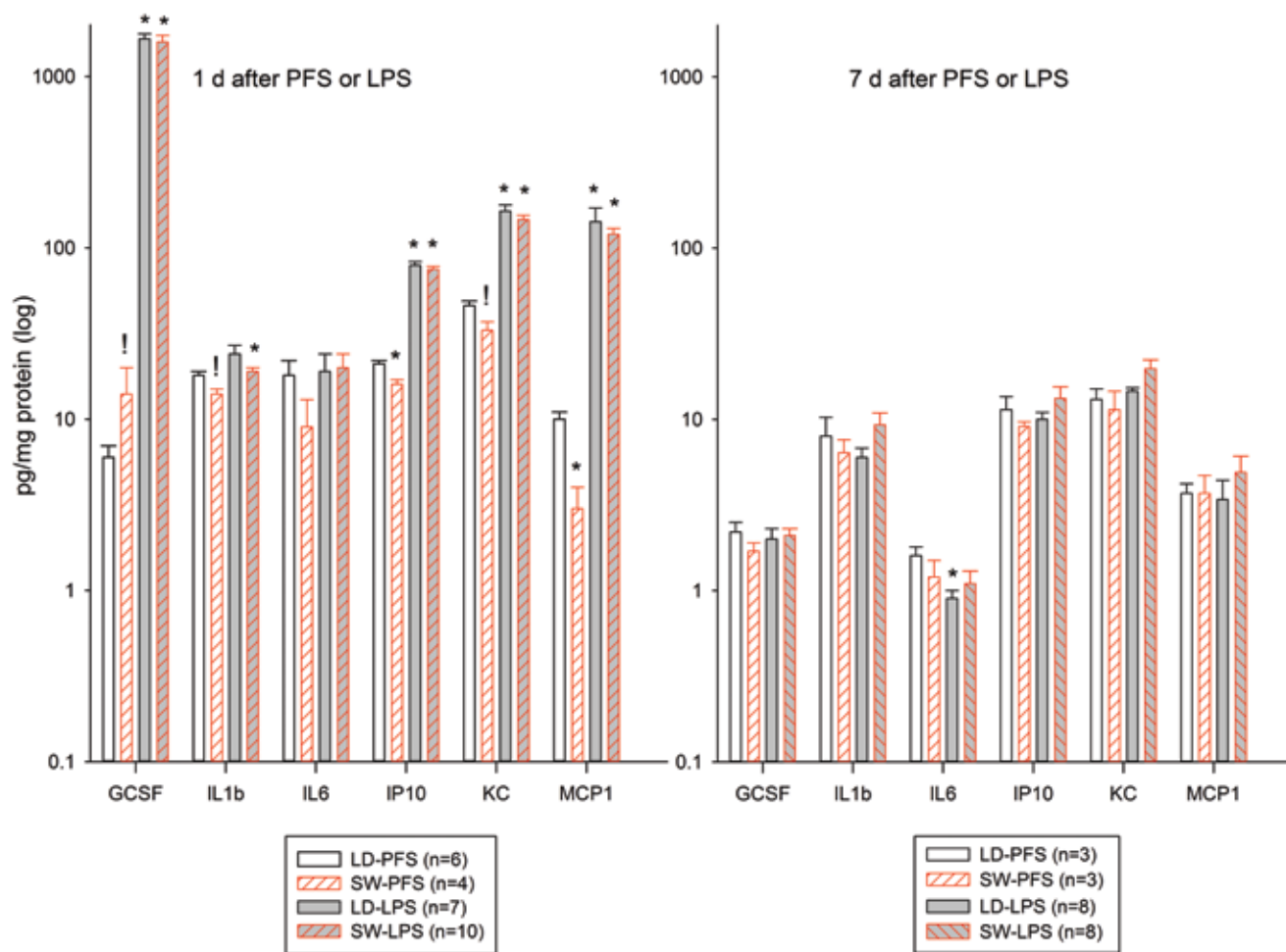


**Figure 5.** Effect of LPS administration on lung cytokine and chemokine concentrations in IFN $\gamma$ KO mice with latent M3FL infection. Female IFN $\gamma$ KO mice with latent M3FL infection were euthanized either 1 d or 7 d after intraperitoneal administration of LPS (15  $\mu$ g) or an equivalent volume of PFS. Lung was collected and immediately frozen for subsequent assay of a panel of cytokines and chemokines by multiplex bead-based assays. \*,  $P \leq 0.01$ ; !,  $0.05 < P < 0.1$  (trend).

that the 7-d time point is associated with viral reactivation after LPS challenge in C57BL/6J mice.<sup>22</sup> On day 7 after treatment, SW mice with latent viral infection and given LPS had greater viral loads (according to both BLI and real-time PCR analysis) than did SW mice given PFS, indicating that exposure to SW increased susceptibility to LPS-induced viral reactivation. At 24 h after LPS administration, concentrations of some cytokines and chemokines in lung were markedly elevated relative to those in PFS-treated mice, but those effects had dissipated by day 7 (Figure 5). Significant decreases and trends toward reduction were observed for some analytes at 24 h after PFS administration in SW- compared with LD-exposed mice. This observation suggests that exposure to simulated SW was associated with a blunting of the host innate response to this microbial challenge. This observation, together with our previous report of prolonged effects of LPS on temperature, locomotor activity, and sleep in MuGHV-infected C57BL/6J mice,<sup>49</sup> suggests that intermediate time points of 3 to 4 d after LPS administration might have revealed prolonged effects on lung cytokine and chemokine concentrations in MuGHV-infected mice. Additional studies are needed to test this hypothesis.

Although we did not measure sleep in the current study, others have documented that repeated diurnal disruption causes both sleep loss and altered inflammatory responses to LPS in mice.<sup>9,11</sup> In people, SW is associated with loss of sleep, increased sleepiness, and an increased likelihood of the occurrence of involuntary sleep.<sup>3,8,57</sup> Like circadian disruption, inadequate sleep has long been associated with increased risk of disease. Considerable evidence indicates that sleep loss, like circadian disruption, is associated with significant perturbation of host immune and inflammatory responses,<sup>6,31,44,53,54,74,76</sup> which likely contribute to enhanced risk, a suboptimal host response to challenge, and prolonged recuperation. In fact, some studies have directly assessed the effect of short sleep duration on susceptibility to infectious challenge and response to immunization in people, generally finding that poor or limited sleep is associated with increased risk and poor responses.<sup>36,53,54,60</sup> Therefore, both sleep loss and circadian disruption, as well as related metabolic and immunologic perturbations, likely contribute to the results we report.

People experiencing viral infections often develop a variety of symptoms that include malaise and fatigue. Generally these symptoms resolve as the person recovers. However, some people continue to experience fatigue long after the infection apparently

resolves. For example, among 140 patients with a history of West Nile virus infection, 31% reported fatigue that lasted for more than 6 mo after infection, with an average duration of 5 y.<sup>21</sup> Some patients with postinfective fatigue may be diagnosed as having a condition called chronic fatigue syndrome, recently renamed Systemic Exertion Intolerance Disease by the Institute of Medicine (<http://www.iom.edu/Reports/2015/ME-CFS.aspx>). In many cases, this illness begins after the patient experiences a flu-like condition. For example, adolescents and young adults who have had mononucleosis can develop fatigue that lasts for a year or more after other symptoms resolve,<sup>32,33,39</sup> with women being more likely than men to develop fatigue. We and others have hypothesized that chronic fatigue occurs because the patient's immune system remains primed or activated even after the acute infection is gone; this residual activation primes the immune system for overreaction to other mild challenges like a minor bacterial infection, exercise, or sleep loss. For example, in patients with chronic fatigue syndrome, over-exercising can intensify symptoms, and some patients experience profound fatigue after even moderate exercise.<sup>28,70</sup> Although the etiology of chronic fatigue syndrome is uncertain and likely viable among patients, a substantial body of evidence suggests an infectious trigger in at least some patient populations.<sup>7,47,75</sup>

In conclusion, our data show that chronic exposure to simulated SW in association with an acute inflammatory challenge (LPS) can reactivate latent virus and increase total viral load in lung of immune-impaired MuGHV-infected mice. Such reactivation might contribute to the associated development of secondary symptoms of infectious disease. The findings offer additional support for the adverse effects of chronic exposure to diurnal disorganization on health. Our study further indicates that the development of these outcomes in a host animal are likely multifactorial in etiology.

## Acknowledgments

This work was supported in part by NIH grant R01-AI080576 and by the Southern Illinois University School of Medicine. We thank Michelle Randle and Megan Ilsley-Woods for technical assistance with this project and Dr Steve Verhulst for consultation on the statistical analysis.

## References

1. **Ablashi DV.** 1994. Summary: viral studies of chronic fatigue syndrome. *Clin Infect Dis* **18** suppl.1:S130–S133.
2. **Agliari E, Barra A, Vidal KG, Guerra F.** 2012. Can persistent Epstein-Barr virus infection induce chronic fatigue syndrome as a Pavlov reflex of the immune response? *J Biol Dyn* **6**:740–762.
3. **Akerstedt T.** 2003. Shift work and disturbed sleep/wakefulness. *Occup Med (Lond)* **53**:89–94.
4. **Aldabal L, Bahammam AS.** 2011. Metabolic, endocrine, and immune consequences of sleep deprivation. *Open Respir Med J* **5**:31–43.
5. **Barton E, Mandal P, Speck SH.** 2011. Pathogenesis and host control of gammaherpesviruses: lessons from the mouse. *Annu Rev Immunol* **29**:351–397.
6. **Besedovsky L, Lange T, Born J.** 2011. Sleep and immune function. *Pflugers Arch* **463**:121–137.
7. **Bested AC, Marshall LM.** 2015. Review of Myalgic Encephalomyelitis/Chronic Fatigue Syndrome: an evidence-based approach to diagnosis and management by clinicians. *Rev Environ Health* **30**:223–249.
8. **Boivin DB, Boudreau P.** 2014. Impacts of shift work on sleep and circadian rhythms. *Pathol Biol (Paris)* **62**:292–301.
9. **Brager AJ, Ehlen JC, Castanon-Cervantes O, Natarajan D, Delisser P, Davidson AJ, Paul KN.** 2013. Sleep loss and the inflammatory response in mice under chronic environmental circadian disruption. *PLoS One* **8**:e63752.
10. **Cardin RD, Brooks JW, Sarawar SR, Doherty PC.** 1996. Progressive loss of CD8<sup>+</sup> T cell-mediated control of a  $\gamma$ -herpesvirus in the absence of CD4<sup>+</sup> T cells. *J Exp Med* **184**:863–871.
11. **Castanon-Cervantes O, Wu M, Ehlen JC, Paul K, Gamble KL, Johnson RL, Besing RC, Menaker M, Gewirtz AT, Davidson AJ.** 2010. Dysregulation of inflammatory responses by chronic circadian disruption. *J Immunol* **185**:5796–5805.
12. **Chen-Goodspeed M, Lee CC.** 2007. Tumor suppression and circadian function. *J Biol Rhythms* **22**:291–298.
13. **Cleare AJ.** 2003. The neuroendocrinology of chronic fatigue syndrome. *Endocr Rev* **24**:236–252.
14. **Coleman SM, McGregor A.** 2015. A bright future for bioluminescent imaging in viral research. *Future Virol* **10**:169–183.
15. **Feced Olmos CM, Fernandez Matilla M, Robustillo Villarino M, de la Morena Barrio I, Alegre Sancho JJ.** 2016. Joint involvement secondary to Epstein-Barr virus. *Reumatol Clin* **12**:100–102. [Article in English, Spanish].
16. **Flano E, Husain SM, Sample JT, Woodland DL, Blackman MA.** 2000. Latent murine  $\gamma$ -herpesvirus infection is established in activated B cells, dendritic cells, and macrophages. *J Immunol* **165**:1074–1081.
17. **Flano E, Kim IJ, Moore J, Woodland DL, Blackman MA.** 2003. Differential  $\gamma$ -herpesvirus distribution in distinct anatomical locations and cell subsets during persistent infection in mice. *J Immunol* **170**:3828–3834.
18. **Flano E, Woodland DL, Blackman MA.** 2002. A mouse model for infectious mononucleosis. *Immunol Res* **25**:201–217.
19. **Francois S, Vidick S, Sarlet M, Desmecht D, Drion P, Stevenson PG, Vanderplasschen A, Gillet L.** 2013. Illumination of murine gammaherpesvirus-68 cycle reveals a sexual transmission route from females to males in laboratory mice. *PLoS Pathog* **9**:e1003292.
20. **Francois S, Vidick S, Sarlet M, Michaux J, Koteja P, Desmecht D, Stevenson PG, Vanderplasschen A, Gillet L.** 2010. Comparative study of murid gammaherpesvirus 4 infection in mice and in a natural host, bank voles. *J Gen Virol* **91**:2553–2563.
21. **Garcia MN, Hause AM, Walker CM, Orange JS, Hasbun R, Murray KO.** 2014. Evaluation of prolonged fatigue postwest Nile virus infection and association of fatigue with elevated antiviral and proinflammatory cytokines. *Viral Immunol* **27**:327–333.
22. **Gargano LM, Forrest JC, Speck SH.** 2008. Signaling through Toll-like receptors induces murine gammaherpesvirus 68 reactivation in vivo. *J Virol* **83**:1474–1482.
23. **Glaser R, Kiecolt-Glaser JK.** 1998. Stress-associated immune modulation: relevance to viral infections and chronic fatigue syndrome. *Am J Med* **105**:35S–42S.
24. **Glaser R, Padgett DA, Litsky ML, Baiocchi RA, Yang EV, Chen M, Yeh PE, Klimas NG, Marshall GD, Whiteside T, Herberman R, Kiecolt-Glaser J, Williams MV.** 2005. Stress-associated changes in the steady-state expression of latent Epstein-Barr virus: implications for chronic fatigue syndrome and cancer. *Brain Behav Immun* **19**:91–103.
25. **Guilleminault C, Mondini S.** 1986. Mononucleosis and chronic daytime sleepiness: a longterm follow-up study. *Arch Intern Med* **146**:1333–1335.
26. **Haus EL, Smolensky MH.** 2013. Shift work and cancer risk: Potential mechanistic roles of circadian disruption, light at night, and sleep deprivation. *Sleep Med Rev* **17**:273–284.
27. **Hwang S, Wu TT, Tong LM, Kim KS, Martinez-Guzman D, Colantonio AD, Uittenbogaart CH, Sun R.** 2008. Persistent gammaherpesvirus replication and dynamic interaction with the host in vivo. *J Virol* **82**:12498–12509.
28. **Jason LA, Sunnquist M, Brown A, Furst J, Cid M, Farietta J, Kot B, Bloomer C, Nicholson L, Williams Y, Jantke R, Newton JL, Strand EB.** 2015. Factor analysis of the DePaul symptom questionnaire: Identifying core domains. *J Neurol Neurobiol* **1**.



29. Jones JF, Williams M, Schooley RT, Robinson C, Glaser R. 1988. Antibodies to Epstein-Barr virus-specific DNase and DNA polymerase in the chronic fatigue syndrome. *Arch Intern Med* **148**:1957–1960.
30. Josephs SF, Henry B, Balachandran N, Strayer D, Peterson D, Komaroff AL, Ablashi DV. 1991. HHV-6 reactivation in chronic fatigue syndrome. *Lancet* **337**:1346–1347.
31. Karatsoreos IN, McEwen BS. 2014. Timing is everything: a collection on how clocks affect resilience in biological systems. *F1000Res* **3**:273.
32. Katz BZ, Jason LA. 2013. Chronic fatigue syndrome following infections in adolescents. *Curr Opin Pediatr* **25**:95–102.
33. Katz BZ, Shiraishi Y, Mears CJ, Binns HJ, Taylor R. 2009. Chronic fatigue syndrome after infectious mononucleosis in adolescents. *Pediatrics* **124**:189–193.
34. Kc R, Li X, Forsyth CB, Voigt RM, Summa KC, Vitaterna MH, Tryniszewska B, Keshavarzian A, Turek FW, Meng QJ, Im HJ. 2015. Osteoarthritis-like pathologic changes in the knee joint induced by environmental disruption of circadian rhythms is potentiated by a high-fat diet. *Sci Rep* **5**:16896.
35. Kc R, Li X, Voigt RM, Ellman RB, Summa KC, Vitaterna MH, Keshavarzian A, Turek FW, Meng QJ, Stein GS, van Wijnen AJ, Chen D, Forsyth CB, Im HJ. 2015. Environmental disruption of circadian rhythm predisposes mice to osteoarthritis-like changes in knee joint. *J Cell Physiol* **230**:2174–2183.
36. Lange T, Perras B, Fehm HL, Born J. 2003. Sleep enhances the human antibody response to hepatitis A vaccination. *Psychosom Med* **65**:831–835.
37. Loebel M, Strohschein K, Gianinni C, Koelsch U, Bauer S, Doebis C, Thomas S, Unterwalder N, von Baehr V, Reinke P, Knops M, Hanitsch LG, Meisel C, Volk HD, Scheibenbogen C. 2014. Deficient EBV-specific B- and T-cell response in patients with chronic fatigue syndrome. *PLoS One* **9**:e85387.
38. Lucassen EA, Rother KI, Cizza G. 2012. Interacting epidemics? Sleep curtailment, insulin resistance, and obesity. *Ann NY Acad Sci* **1264**:110–134.
39. Macsween KF, Higgins CD, McAulay KA, Williams H, Harrison N, Swerdlow AJ, Crawford DH. 2010. Infectious mononucleosis in university students in the United Kingdom: evaluation of the clinical features and consequences of the disease. *Clin Infect Dis* **50**:699–706.
40. Maywood ES, O'Neill J, Wong GK, Reddy AB, Hastings MH. 2006. Circadian timing in health and disease. *Prog Brain Res* **153**:253–269.
41. Mehraein Y, Lennerz C, Ehlhardt S, Remberger K, Ojak A, Zang KD. 2004. Latent Epstein-Barr virus (EBV) infection and cytomegalovirus (CMV) infection in synovial tissue of autoimmune chronic arthritis determined by RNA- and DNA-in situ hybridization. *Mod Pathol* **17**:781–789.
42. Milho R, Smith CM, Marques S, Alenquer M, May JS, Gillet L, Gaspar M, Efstathiou S, Simas JP, Stevenson PG. 2009. In vivo imaging of murid herpesvirus-4 infection. *J Gen Virol* **90**:21–32.
43. Morris CJ, Yang JN, Scheer FA. 2012. The impact of the circadian timing system on cardiovascular and metabolic function. *Prog Brain Res* **199**:337–358.
44. Mullington JM, Simpson NS, Meier-Ewert HK, Haack M. 2010. Sleep loss and inflammation. *Best Pract Res Clin Endocrinol Metab* **24**:775–784.
45. Natelson BH, Ye N, Moul DE, Jenkins FJ, Oren DA, Tapp WN, Cheng YC. 1994. High titers of anti-Epstein-Barr virus DNA polymerase are found in patients with severe fatiguing illness. *J Med Virol* **42**:42–46.
46. Nea FM, Kearney J, Livingstone MB, Pourshahidi LK, Corish CA. 2015. Dietary and lifestyle habits and the associated health risks in shift workers. *Nutr Res Rev* **28**:143–166.
47. Nijs J, Nees A, Paul L, De Koning M, Ickmans K, Meeus M, Van Oosterwijck J. 2014. Altered immune response to exercise in patients with chronic fatigue syndrome/myalgic encephalomyelitis: a systematic literature review. *Exerc Immunol Rev* **20**:94–116.
48. Olivadoti M, Toth LA, Weinberg J, Opp MR. 2007. Murine gammaherpesvirus: a model for the study of Epstein-Barr virus infection and related diseases. *Comp Med* **57**:44–50.
49. Olivadoti MD, Weinberg JB, Toth LA, Opp MR. 2011. Sleep and fatigue in mice infected with murine gammaherpesvirus 68. *Brain Behav Immun* **25**:696–705.
50. Olivier J, Johnson JWD, Marshall GD. 2008. The logarithmic transformation and the geometric mean in reporting experimental IgE results: what are they and when and why to use them? *Ann Allergy Asthma Immunol* **100**:333–337.
51. Pan A, Schernhammer ES, Sun Q, Hu FB. 2011. Rotating night shift work and risk of type 2 diabetes: two prospective cohort studies in women. *PLoS Med* **8**:e1001141.
52. Papanicolaou DA, Amsterdam JD, Levine S, McCann SM, Moore RC, Newbrand CH, Allen G, Nisenbaum R, Pfaff DW, Tsokos GC, Vgontzas AN, Kales A. 2004. Neuroendocrine aspects of chronic fatigue syndrome. *Neuroimmunomodulation* **11**:65–74.
53. Prather AA, Hall M, Fury JM, Ross DC, Muldoon MF, Cohen S, Marsland AL. 2012. Sleep and antibody response to hepatitis B vaccination. *Sleep* **35**:1063–1069.
54. Prather AA, Janicki-Deverts D, Hall MH, Cohen S. 2015. Behaviorally assessed sleep and susceptibility to the common cold. *Sleep* **38**:1353–1359.
55. Qian J, Scheer FA. 2016. Circadian system and glucose metabolism: Implications for physiology and disease. *Trends Endocrinol Metab* **27**:282–293.
56. Rajaratnam SM, Arendt J. 2001. Health in a 24-h society. *Lancet* **358**:999–1005.
57. Rajaratnam SM, Howard ME, Grunstein RR. 2013. Sleep loss and circadian disruption in shift work: health burden and management. *Med J Aust* **199**:11–15.
58. Reutrakul S, Knutson KL. 2015. Consequences of circadian disruption on cardiometabolic health. *Sleep Med Clin* **10**:455–468.
59. Sarawar SR, Cardin RD, Brooks JW, Mehrpooya M, Hamilton-Easton AM, Mo XY, Doherty PC. 1997. Gamma interferon is not essential for recovery from acute infection with murine gammaherpesvirus 68. *J Virol* **71**:3916–3921.
60. Spiegel K, Sheridan JF, Van Cauter E. 2002. Effect of sleep deprivation on response to immunization. *JAMA* **288**:1471–1472.
61. Steed A, Buch T, Waisman A, Virgin HW 4th. 2007. Gamma interferon blocks gammaherpesvirus reactivation from latency in a cell type-specific manner. *J Virol* **81**:6134–6140.
62. Stevenson PG, Simas JP, Efstathiou S. 2009. Immune control of mammalian  $\gamma$ -herpesviruses: lessons from murid herpesvirus-4. *J Gen Virol* **90**:2317–2330.
63. Sunil-Chandra NP, Efstathiou S, Nash AA. 1992. Murine gamma-herpesvirus 68 establishes a latent infection in mouse B lymphocytes in vivo. *J Gen Virol* **73**:3275–3279.
64. Takeda T, Mizugaki Y, Matsubara L, Imai S, Koike T, Takada K. 2000. Lytic Epstein-Barr virus infection in the synovial tissue of patients with rheumatoid arthritis. *Arthritis Rheum* **43**:1218–1225.
65. Tobi M, Strauss SE. 1988. Chronic mononucleosis - a legitimate diagnosis. *Postgrad Med* **83**:69–78.
66. Trammell RA, Toth LA. 2015. Effects of sleep fragmentation and chronic latent viral infection on behavior and inflammation in mice. *Comp Med* **65**:173–185.
67. Trammell RA, Verhulst S, Toth LA. 2014. Effects of sleep fragmentation on sleep and markers of inflammation in mice. *Comp Med* **64**:13–24.
68. Truong KK, Lam MT, Grandner MA, Sassoos CS, Malhotra A. 2016. Timing matters: circadian rhythm in sepsis, obstructive lung disease, obstructive sleep apnea, and cancer. *Ann Am Thorac Soc* **13**:1144–1154.
69. Tsai CY, Hu Z, Zhang W, Usherwood EJ. 2011. Strain-dependent requirement for IFN- $\alpha$  for respiratory control and immunotherapy in murine gammaherpesvirus infection. *Viral Immunol* **24**:273–280.

70. **Twisk FN.** 2015. Accurate diagnosis of myalgic encephalomyelitis and chronic fatigue syndrome based upon objective test methods for characteristic symptoms. *World J Methodol* 5:68–87.
71. **Vyas MV, Garg AX, Iansavichus AV, Costella J, Donner A, Laugsand LE, Janszky I, Mrkobrada M, Parranga G, Hackam DG.** 2012. Shift work and vascular events: systematic review and meta-analysis. *BMJ* 345:e4800.
72. **Weinberg JB, Lutzke ML, Alfinito R, Rochford R.** 2004. Mouse strain differences in the chemokine response to acute lung infection with a murine gammaherpesvirus. *Viral Immunol* 17:69–77.
73. **White PD, Thomas JM, Amess J, Crawford DH, Grover SA, Kangro HO, Clare AW.** 1998. Incidence, risk and prognosis of acute and chronic fatigue syndromes and psychiatric disorders after glandular fever. *Br J Psychiatry* 173:475–481.
74. **Wright KP Jr, Drake AL, Frey DJ, Fleshner M, Desouza CA, Gronfier C, Czeisler CA.** 2015. Influence of sleep deprivation and circadian misalignment on cortisol, inflammatory markers, and cytokine balance. *Brain Behav Immun* 47:24–34.
75. **Zhang L, Gough J, Christmas D, Matthey DL, Richards SC, Main J, Enlander D, Honeybourne D, Ayres JG, Nutt DJ, Kerr JR.** 2009. Microbial infections in 8 genomic subtypes of chronic fatigue syndrome/myalgic encephalomyelitis. *J Clin Pathol* 63:156–164.
76. **Zielinski MR, Krueger JM.** 2011. Sleep and innate immunity. *Front Biosci (Schol Ed)* 3:632–642.